MEaSUREs (Making Earth System Data Records for Use in Research Environments)

Geosynchronous Land Surface Temperature Product (GEO-LST) User Guide

Kerry Cawse-Nicholson[1], Simon Hook[1], Glynn Hulley[1], Rachel Pinker[2]

[1]Jet Propulsion Laboratory, California Institute of Technology
[2]University of Maryland

National Aeronautics and

Space Administration

Jet Propulsion Laboratory
California Institute of Technology
Pasadena, California

January 2020

This research was carried out at the Jet Propulsion Laboratory, California Institute of Technology, under a contract with the National Aeronautics and Space Administration.

Reference herein to any specific commercial product, process, or service by trade name, trademark, manufacturer, or otherwise, does not constitute or imply its endorsement by the United States Government or the Jet Propulsion Laboratory, California Institute of Technology.

© 2020. California Institute of Technology. Government sponsorship acknowledged.

Change History Log

Revision	Effective Date	Prepared by	Description of Changes
1.0	12/17/2019	Kerry Cawse-Nicholson	User Guide first draft
1.1	1/8/2020	Glynn Hulley	Updates to cloud and uncertainty sections

Contacts

Readers seeking additional information about this product may contact the following:

- Kerry Cawse-Nicholson
  MS 183-501
  Jet Propulsion Laboratory
  4800 Oak Grove Dr.
  Pasadena, CA 91109
  Email: kcawseni@jpl.nasa.gov
  Office: (818) 354-1594

Contents

List of figures

List of tables

1 Introduction

This is the user guide for the MEaSUREs (Making Earth System Data Records for Use in Research Environments) Land Surface Temperature (LST) product derived from the Geostationary Operational Environmental Satellite (GOES) satellite data record. The GEO-LST product will include LST produced hourly over North and South America for GOES-8 through GOES-15 satellites since 2000. This is version 1.0 of the ATBD and the goal is maintaining a 'living' version of this document with changes made when necessary.

Land Surface Temperature and Emissivity (LST&E) are critical variables used in a wide range of Earth science studies. They are necessary inputs for surface energy balance models used in drought monitoring, soil moisture estimation, and monitoring water consumptive use (Anderson et al. 2011a; Hain et al. 2011; Semmens et al. 2016). They are used for the retrieval of climate variables such as tropospheric water vapor and air temperature (Seemann et al. 2008; Susskind and Blaisdell 2008; Yao et al. 2011). They are also used to monitor climate warming trends (Hall et al. 2012; Schneider and Hook 2010), measure the urban heat island effect (Dousset and Gourmelon 2003; Luvall et al. 2015) and heat waves (Dousset et al. 2011; Luvall et al. 2015), detect land cover and land use change (French et al. 2008; Hulley et al. 2014a), and map surface composition (Hook et al. 2005; Vaughan et al. 2005).

NASA has identified LST&E data as an important Earth System Data Record (ESDR) (NASA 2005, 2011) along with other international organizations (e.g. Global Climate Observing System (GCOS), 2003; Climate Change Science Program (CCSP), 2006). LST was recently designated as an Essential Climate Variable (ECV) by GCOS and several international initiatives have been established to utilize LST&E data including the EarthTemp network (http://www.earthtemp.net/), GlobTemperature (http://www.globtemperature.info/) and the International Land Surface Temperature and Emissivity Working Group (ILSTE-WG, http://ilste-wg.org/).

LST&E products are routinely produced by NASA and NOAA from sensors in low earth orbit (LEO) from the Moderate Resolution Imaging Spectroradiometer (MODIS) and Visible Infrared Imaging Radiometer Suite (VIIRS) sensors on board the Aqua (2002)/Terra (2000) and Suomi-NPP (2011) platforms respectively. LST products are also produced from sensors in geostationary Earth orbit (GEO) such as the Geostationary Operational Environmental Satellites (GOES). Sensors in LEO orbits provide global coverage at moderate spatial resolutions (~1km) but more limited temporal coverage (up to twice-daily), while sensors in GEO orbits provide more frequent measurements (hourly) at lower spatial resolutions (~2-4 km) over a geographically restricted area. For example, the GOES sensors produce data over North America every 15 minutes and South America every 3 hours. However, these sensor-based LST&E products are generated with varying accuracies depending on the input data, including ancillary data such as atmospheric water vapor, as well as algorithmic approaches. They are also on different space-time grids and lack full uncertainty information limiting their usefulness for many studies. Our current project was selected to address these limitations by creating a set of unified and coherent LST&E products and this follow-on work will develop and extend these products. LST&E data are used for many Earth surface related studies such as surface energy balance modeling (Zhou et al. 2003b) and land-cover land-use change detection (French et al. 2008), while they are also critical for accurately retrieving important climate variables such as air temperature and relative humidity (Yao et al. 2011). The LST is an important long-term climate indicator, and a key variable for drought monitoring over arid lands (Anderson et al. 2011a; Rhee

et al. 2010). The LST is an input to ecological models that determine important variables used for water use management such as evapotranspiration and soil moisture (Anderson et al. 2011b).

GEO LST products produced from GOES are currently available through NOAA OSPO (http://www.ospo.noaa.gov/Products/land/glst/) but are produced using different retrieval algorithms throughout the GOES record, e.g. GOES sensors 8-11 use a split-window algorithm, while GOES sensors 12-14 use a single channel algorithm (since the 11-12 micron band combination necessary for the split-window was not available for these sensors). This results in a discontinuity in the retrieval record and affects the accuracy of the GOES LST time series beginning with GOES 12. To address this issue, we developed a GEO-LST product using a consistent single-channel GOES algorithm applicable to all GOES sensors from GOES 8-16 and onward. The algorithm uses a radiative transfer approach for the atmospheric correction similar to the MxD21 approach, combined with an improved Combined ASTER and MODIS Emissivity for Land (CAMEL) emissivity data record for the emissivity correction (https://lpdaac.usgs.gov/products/cam5k30emv002/). The GEO-LST product merges six generations of GOES sensors and instrument characteristics.

1.1 File format for L3 products

The GEO-LST products are distributed in HDF5 format and can be read in by HDF5 software. Information on Hierarchical Data Format 5 (HDF5) may be found at https://www.hdfgroup.org/HDF5/. The HDF format was developed by NCSA and has been widely used in the scientific domain. HDF5 can store two primary types of objects: datasets and groups. A dataset is essentially a multidimensional array of data elements, and a group is a structure for organizing objects in an HDF5 file. HDF5 was designed to address some of the limitations of the HDF4. Using these two basic objects, one can create and store almost any kind of scientific data structure, such as images, arrays of vectors, and structured and unstructured grids. They can be mixed and matched in HDF5 files according to user needs. HDF5 does not limit the size of files or the size or number of objects in a file. The scientific data results are delivered as SDSs with local attributes including summary statistics and other information about the data.

The GEO-LST data product files contain one set of Attributes (metadata) describing information relevant to production, archiving, user services, input products, geolocation and analysis of data, as well as provenance and Digital Object Identifier (DOI) of the product attached to the root group (the file). The attributes listed in Table 4 are not described further in this user guide.

1.2 GEO-LST Product

The GEO-LST data product is produced for GOES North America Extended spatial range (see Figure 1), in swath format, yielding estimates of hourly land surface temperature. The spatial resolution of each pixel is 4x4 km.

1.3 Product Availability

The GEO-LST product will be made available at the NASA Land Processes Distributed Active Archive Center (LPDAAC), https://earthdata.nasa.gov/ and can be accessed via the Earthdata search engine.

2 GEO-LST Product

2.1 Algorithm Description

The basic processing steps involved in GEO-LST product generation are outlined schematically in Fig. 2, and a list of the inputs is listed in Table 1. (for a full detailed description of the GEO-LST processing scheme please see the ATBD).

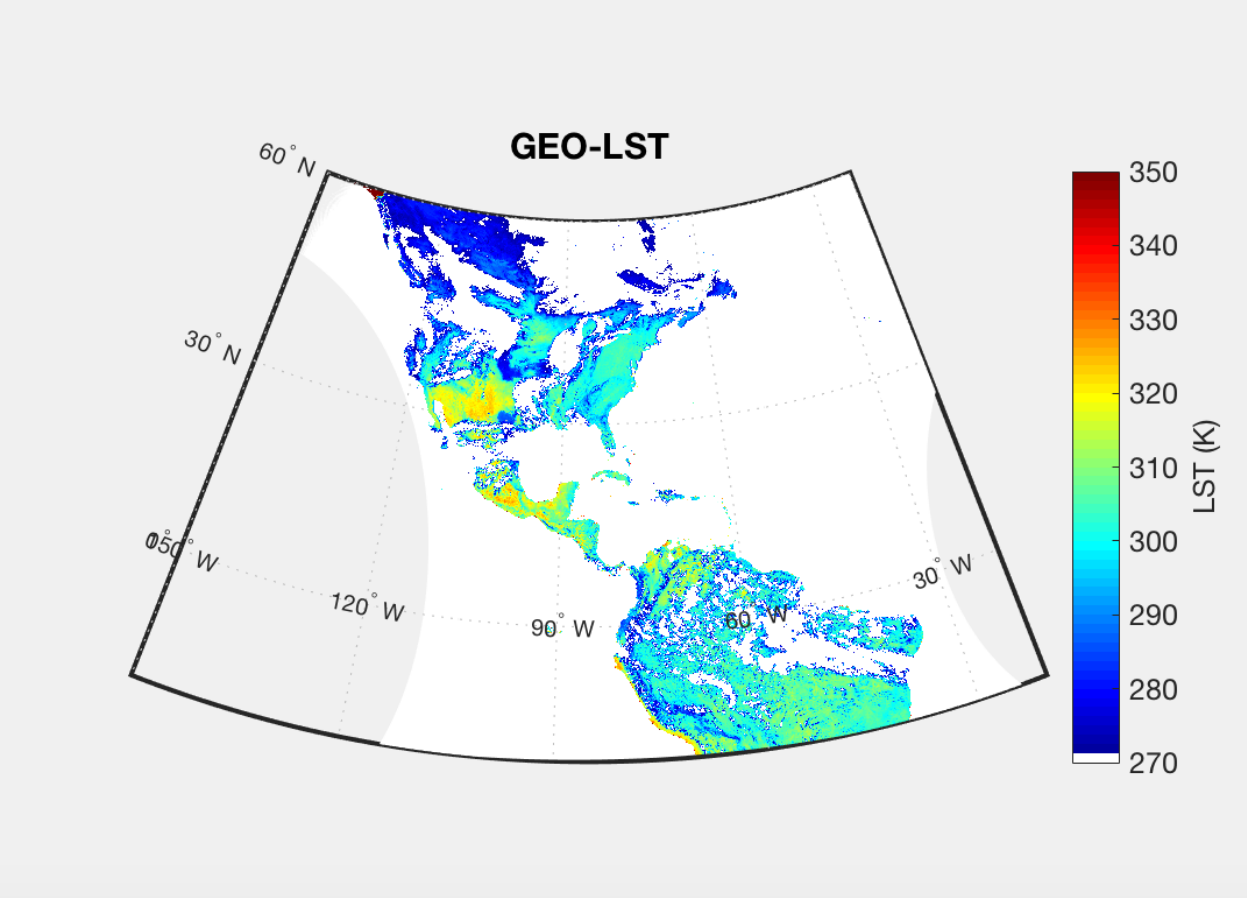

Figure 1. A sample a cloud-screened GEO-LST image acquired on 4/28/2003 at 1815UTC.

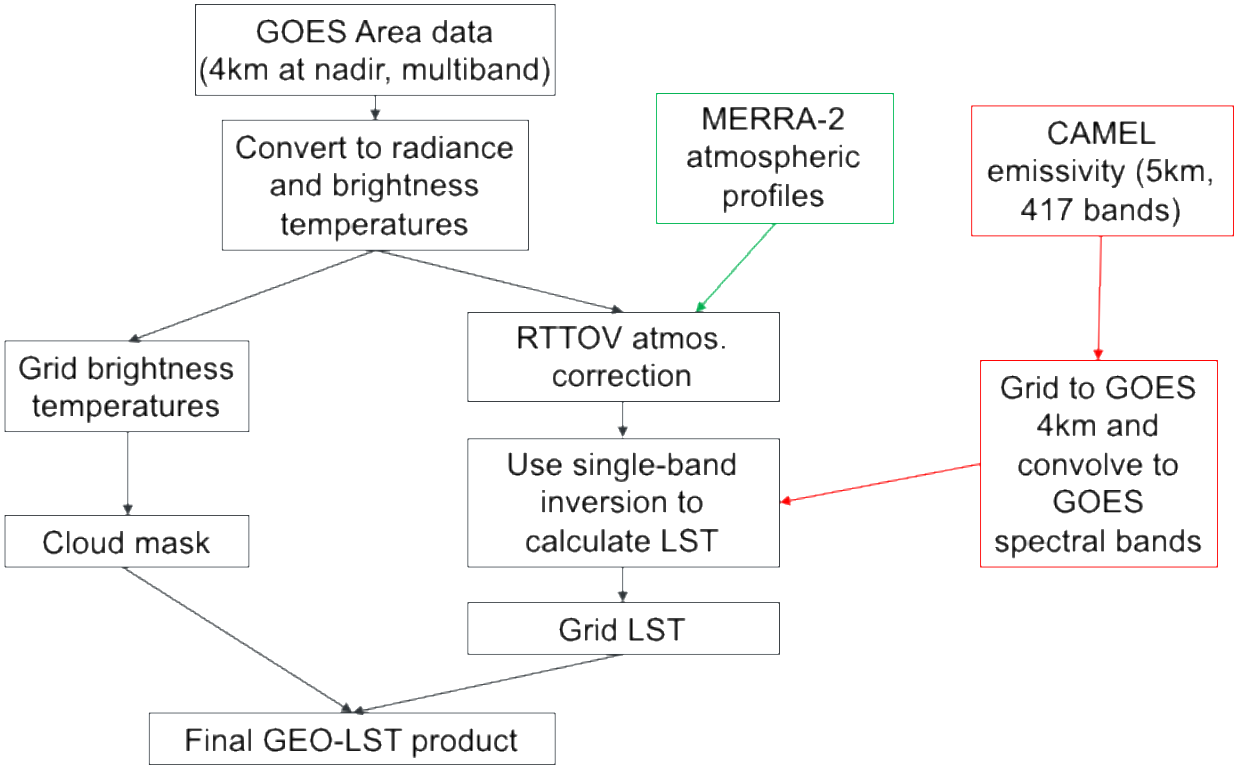

Figure 2. Conceptual diagram describing computation of GEO-LST.

Table 1: Input products and ancillary data required to produce the GEO-LST product.

Ancillary Data Set	**Long Name**	**Data Used**
GOES	GOES imager	Radiance
MERRA-2	MERRA-2 atmospheric profiles	Pressure Air Temperature Specific Humidity Surface Pressure
CAMEL	CAMEL emissivity	Longwave emissivity

2.2 Scientific Data Sets (SDS)

The GEO-LST product contains 5 scientific data sets (SDSs): cloud mask, latitude, longitude, land surface temperature, and associated error. All SDS data are output on a GOES swath, at 4km resolution at nadir. Details of each SDS including data type and units are shown in Table 2, and the associated attributes of each SDS is shown in Table 3.

Table 2. The Scientific Data Sets (SDS) in the GEO-LST product.

Field Name	Type	Unit	Scaling
cloud	Uint8	n/a	n/a
lat	Float	Decimal degrees	n/a
lon	Float	Decimal degrees	n/a
lst	int16	Kelvin	Scale = 0.02
lst_err	int8	Kelvin	Scale = 0.04

Table 3. The attributes assigned to each dataset.

Field Name	Type	Unit	Field Data
long_name	string		
units	string		
Format	String		scaled
coordsys	string		cartesian
Valid_range	Float		
_FillValue	Float		
_Scale	Float		
_Offset	Float		

2.3 Attributes

Archived with the SDS are attributes (metadata) describing characteristics of the data. Contents of these attributes were determined and written during generation of the product at JPL and are used in archiving and populating the database at the LPDAAC to support user services. They are stored as very long character strings in parameter value language (PVL) format. Descriptions of the attributes are given here to assist the user in understanding them. The product specific metadata in Table 4 give details on ancillary data sets.

Table 4. Standard attributes included in all GEO-LST products.

Name	Type	Size	Example
AlgorithmVersion	String	variable	
DataResolution	String	variable	4km
DayNightFlag	String	variable	n/a
EastBoundingCoordinate	LongFloat	8	
IdentifierProductDOI	String	variable	10.5067/MEaSUREs/LSTE/GEOLST4KHR.001
IdentifierProductDOIAuthority	String	variable	https:/doi.org
LocalGranuleID	String	variable	
LongName	String	variable	Geostationary Earth Orbit Land Surface Temperature Hourly Global 4KM V001
NorthBoundingCoordinate	LongFloat	8	

PlatformShortName	String	variable	e.g. GOES 08
ProductionTime	String	variable	
Project	String	variable	MEaSUREs
RangeBeginningDate	String	variable	
RangeBeginningTime	String	variable	
SatelliteInstrument	String	variable	Imager
ShortName	String	variable	GEOLST4KHR
VersionID	String	variable	
SouthBoundingCoordinate	LongFloat	8	
WestBoundingCoordinate	LongFloat	8	

2.4 Cloud Mask

The cloud mask is output as a bit mask consisting of a series of cloud threshold tests using a combination of midwave infrared and thermal infrared GOES bands defined in Table 5. Users can use a combination of individual tests to classify clouds, or use bit 5 as a confidence value, where bit 5 represents the total number of positive tests of all the cloud tests used (max value is 3). However, the user may also define their own confidence level based on the five individual cloud tests shown in Table 5. The cloud tests are all based on standard tests used the heritage MODIS cloud mask (MOD35) (Ackerman et al. 2006). Five different tests are employed depending on the GOES sensor that are summarized below:

2.4.1 Thermal brightness test (10.7 µm)

This filter examines the thermal band 10.7 µm brightness temperature to flag potential cloud pixels. Thresholds of 297.5 K and 292.5 K are set for day and nighttime respectively. To account for temperature changes with elevation, a standard lapse rate (6 K/km) is used to calculate an estimate of the changes to the thresholds based on elevation. This test is used for all GOES sensors since they all have channel 4 (10.7 µm).

2.4.2 High cloud test (6.75 µm)

The brightness temperature at 6.75 µm is used to detect thick clouds at or above the 200-500 hPa level. A threshold setting of 225 K is used for this test. This test is used for all GOES sensors since they all have channel 3 (6.7 µm for GOES 8-11 and 6.5 µm for GOES 12-15).

2.4.3 Brightness temperature difference test 1 (10.7 – 3.9 µm)

The brightness temperature difference between window bands 10.7 µm and 3.9 µm can be used to detect the presence of partial or thin cloud for GOES pixels. Thresholds depend on day/night as well as surface type since during the daytime reflected solar radiation will be much higher at 3.9 µm, especially over deserts and semi-arid regions. Different thresholds are set for desert, non-desert land, and water surfaces. Desert pixels are distinguished using the ASTER Global Emissivity Dataset (GEDv3), while water/land pixels are distinguished using a land-water mask. This test is used for all GOES sensors since they all have channel 2 (3.9 µm) and 4 (10.7 µm).

2.4.4 Brightness temperature difference test 2 (11 – 12 µm)

Differences between brightness temperatures in bands 10.7 µm and 3.9 µm have been widely used for cloud screening for MODIS, AVHRR, GOES, and ASTER instruments. The test is often referred to as the split-window technique and relies on differences in optical thickness between the two longwave bands and the non-linear nature of the Planck function. Thresholds are set via a look-up table and depend on satellite view angle and brightness temperature and pre-computed from a dataset of clear-sky radiances. This test is only used for GOES 8-11 since GOES 12-15 do not have the 12 µm band.

2.4.5 CO2 band test for high clouds (13.3 µm)

Brightness temperatures in the CO2 absorption region of 13.3 µm can be used as a simple test to detect cold clouds above 500 hPa. Based on observations of clear-sky radiances at this wavelength we set a threshold of 250 K to distinguish clouds. This test is only available for GOES 12-15 that have the CO2 band (channel 6, 13.3 µm).

Table 5. Cloud mask bit values (fill value = 2^7).

Bit Field	**Long Name**	**Result**
0	Thermal Brightness Test	0 = no 1 = yes
1	Brightness temperature difference test 1 (10.7 – 3.9 µm)	0 = no 1 = yes
2	CO2 band test for high clouds (13.3 µm)	0 = no 1 = yes
3	High cloud test (6.75 µm)	0 = no 1 = yes
4	Brightness temperature difference test 2 (11 – 12 µm)	0 = no 1 = yes
5	Number of positive cloud tests	Number of tests with positive results (max 3)

2.5 LST uncertainty

From previously funded work under the ESDR Uncertainty Analysis Program (ROSES-10), we developed the capability to accurately estimate uncertainties in LST products for a variety of different retrieval algorithms using a Temperature Emissivity Uncertainty Simulator (TEUSim) (Hulley et al. 2012). This model outputs errors in LST due to 1) algorithm error, 2) radiometric noise, 3) atmospheric correction, 4) undetected cloud, and 5) calibration error. The total

uncertainties generated from TEUSim were then parameterized according to satellite view angle (SVA), total water vapor column (TCW), and surface type using a least squares method fit to a quadratic function as follows:

$$\delta LST_{GOES} = a_o + a_1 TCW + a_2 \mathrm{SVA} + a_3 TCW \cdot SVA + a_4 TCW^2 + a_5 SVA^2 \qquad (1)$$

Where δLST is the LST uncertainty (K) and a_i are the land cover dependent regression coefficients. Using this parameterization LST uncertainties can be estimated on a pixel-by-pixel basis for any given sensor. Examples of LST uncertainties produced from this model for GOES-16 are shown in Figure 1-4 for corresponding LSTmin and LSTmax values. LST uncertainties associated with the GEO-LST product will be propagated to the Tair product using a sensitivity study described below.

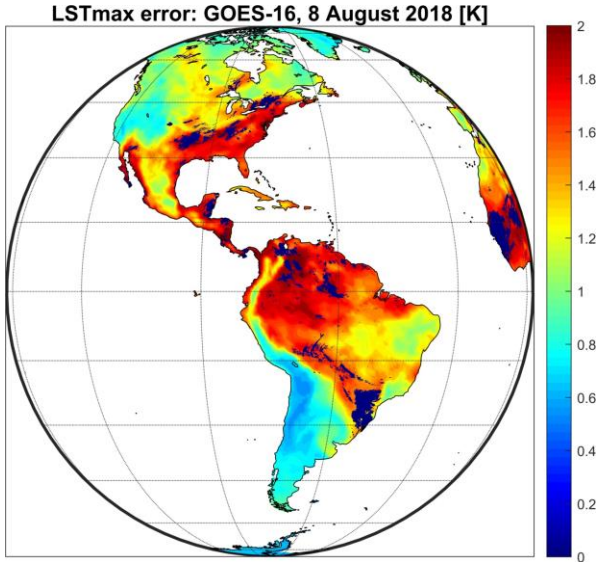

Figure 3. Estimated LST error using equation 1 for a GOES 16 observation on 8 August 2018 at local noon (LSTmax). Areas with high uncertainty (>1.5 K) correspond to regions with high total water vapor loading.

3 References

Ackerman, S., Strabala, K.I., Menzel, P., Frey, R., Moeller, C.C., Gumley, L.E., Baum, B., Seemann, S.W., & Zhang, H. (2006). Discriminating clear-sky from cloud with MODIS

algorithm theoretical basis document (MOD35), *Cooperative Institute for Meteorological Satellite Studies, University of Wisconsin-Madison, NOAA/NESDIS, version 5.0, October 2006*

Anderson, M.C., Hain, C.R., Wardlow, B., Mecikalski, J.R., & Kustas, W.P. (2011a). Evaluation of a drought index based on thermal remote sensing of evapotranspiration over the continental U.S. *Journal of Climate, 24*, 2025-2044

Anderson, M.C., Kustas, W.P., Norman, J.M., Hain, C.R., Mecikalski, J.R., Schultz, L., Gonzalez-Dugo, M.P., Cammalleri, C., d'Urso, G., Pimstein, A., & Gao, F. (2011b). Mapping daily evapotranspiration at field to continental scales using geostationary and polar orbiting satellite imagery. *Hydrology and Earth System Sciences*, *15*, 223-239

Dousset, B., & Gourmelon, F. (2003). Satellite multi-sensor data analysis of urban surface temperatures and landcover. *Isprs Journal of Photogrammetry and Remote Sensing*, 58, 43-54

Dousset, B., Gourmelon, F., Laaidi, K., Zeghnoun, A., Giraudet, E., Bretin, P., Mauri, E., & Vandentorren, S. (2011). Satellite monitoring of summer heat waves in the Paris metropolitan area. *International Journal of Climatology*, 31, 313-323

French, A.N., Schmugge, T.J., Ritchie, J.C., Hsu, A., Jacob, F., & Ogawa, K. (2008). Detecting land cover change at the Jornada Experimental Range, New Mexico with ASTER emissivities. *Remote Sensing of Environment, 112*, 1730-1748

Hain, C.R., Crow, W.T., Mecikalski, J.R., Anderson, M.C., & Holmes, T. (2011). An intercomparison of available soil moisture estimates from thermal infrared and passive microwave remote sensing and land surface modeling. *Journal of Geophysical Research-Atmospheres*, 116

Hall, D.K., Comiso, J.C., DiGirolamo, N.E., Shuman, C.A., Key, J.R., & Koenig, L.S. (2012). A Satellite-Derived Climate-Quality Data Record of the Clear-Sky Surface Temperature of the Greenland Ice Sheet. *Journal of Climate*, 25, 4785-4798

Hook, S.J., Dmochowski, J.E., Howard, K.A., Rowan, L.C., Karlstrom, K.E., & Stock, J.M. (2005). Mapping variations in weight percent silica measured from multispectral thermal infrared imagery - Examples from the Hiller Mountains, Nevada, USA and Tres Virgenes-La Reforma, Baja California Sur, Mexico. *Remote Sensing of Environment, 95*, 273-289

Hulley, G., Veraverbeke, S., & Hook, S. (2014). Thermal-based techniques for land cover change detection using a new dynamic MODIS multispectral emissivity product (MOD21). *Remote Sensing of Environment*, 140, 755-765

Luvall, J., Quattrochi, D.A., Rickman, D., & Estes, M.G. (Eds.) (2015). Urban Heat Islands: Encyclopedia of Atmospheric Sciences

NASA (2005). Exploring our Planet for the Benefit of Society, NASA Earth Science and Applications from Space, Strategic Roadmap, http://images.spaceref.com/news/2005/earth_roadmap.pdf

NASA (2011). NASA Earth Science Data Records Programs, http://science.nasa.gov/earth-science/earth-science-data/Earth-Science-Data-Records-Programs/#ESDR_uncertainty_analysis

Rhee, J., Im, J., & Carbone, G.J. (2010). Monitoring agricultural drought for arid and humid regions using multi-sensor remote sensing data. *Remote Sensing of Environment, 114*, 2875-2887

Schneider, P., & Hook, S.J. (2010). Space observations of inland water bodies show rapid surface warming since 1985. *Geophysical Research Letters*, 37

Seemann, S.W., Borbas, E.E., Knuteson, R.O., Stephenson, G.R., & Huang, H.L. (2008). Development of a global infrared land surface emissivity database for application to clear sky sounding retrievals from multispectral satellite radiance measurements. *Journal of Applied Meteorology and Climatology, 47*, 108-123

Semmens, K.A., Anderson, M.C., Kustas, W.P., Gao, F., Alfieri, J.G., McKee, L., Prueger, J.H., Hain, C.R., Cammalleri, C., Yang, Y., Xia, T., Sanchez, L., Alsina, M.M., & Velez, M. (2016). Monitoring daily evapotranspiration over two California vineyards using Landsat 8 in a multi-sensor data fusion approach. *Remote Sensing of Environment*, 185, 155-170

Susskind, J., & Blaisdell, J. (2008). Improved surface parameter retrievals using AIRS/AMSU data. Proc. SPIE, 6966, DOI: 10.1117/1112.774759

Vaughan, R.G., Hook, S.J., Calvin, W.M., & Taranik, J.V. (2005). Surface mineral mapping at Steamboat Springs, Nevada, USA, with multi-wavelength thermal infrared images. *Remote Sensing of Environment, 99*, 140-158

Yao, Z.G., Li, J., Li, J.L., & Zhang, H. (2011). Surface Emissivity Impact on Temperature and Moisture Soundings from Hyperspectral Infrared Radiance Measurements. *Journal of Applied Meteorology and Climatology, 50*, 1225-1235